Supporting information for

Thermal and Near-Infrared Light Induced Spin Crossover in a Mononuclear Iron(II) Complex with a Tetrathiafulvalene-Fused Dipyridophenazine Ligand

Fabrice Pointillart,[a*] Xunshan Liu,[b] Mikaël Kepenekian,[a] Boris Le Guennic,[a] Stéphane Golhen,[a] Vincent Dorcet,[a] Thierry Roisnel,[a] Olivier Cador,[a] Zhonglu You,[bc] Jürg Hauser,[b] Silvio Decurtins,[b] Lahcène Ouahab[a], Shi-Xia Liu[b*]

[a] Institut des Sciences Chimiques de Rennes, UMR 6226 CNRS - Université de Rennes 1, 263 Avenue du Général Leclerc 35042 Rennes Cedex.
[b] Departement für Chemie und Biochemie, Universität Bern, Freiestrasse 3, CH-3012 Bern, Switzerland.
[c] Present address: Department of Chemistry and Chemical Engineering, Liaoning Normal University, Dalian 116029, P.R. China.

Experimental Section

Crystallography. Single crystal of **1**·(CH$_2$Cl$_2$)$_{1.5}$·(H$_2$O) was mounted on a APEXII Bruker-AXS diffractometer (MoK$_\alpha$ radiation source, λ =0.71073 Å, T = 150(2) K) for data collection from the Centre de Diffractométrie (CDIFX), Université de Rennes 1, France. Structures were solved with a direct method using the SIR-97 program and refined with a full matrix least-squares method on F^2 using the SHELXL-2014 program.[1] Complete crystal structure results as a CIF file including bond lengths, angles, and atomic coordinates are deposited as Supporting Information.

Physical Measurements. Elemental analysis (C, H, N) of the compounds **1**·(CH$_2$Cl$_2$)$_2$ and **1** were performed at the Centre Régional de Mesures Physiques de l'Ouest, Rennes. Optical absorption spectra were recorded on a Varian Cary 5000 UV-Visible-NIR spectrometer

equipped with an integration sphere. The dc magnetic susceptibility measurements were performed on grinded selected single crystals (for **1**·(CH$_2$Cl$_2$)$_2$) and powder (for **1**) in Teflon tape with a Quantum Design MPMS-XL SQUID magnetometer between 2 and 300 K in applied magnetic field of 0.02 T in the temperature range 2-20 K, 0.2 T in the temperature range 20-80 K and 1 T above 80 K. These measurements were all corrected for the diamagnetic contribution of the Teflon tape and the intrinsic diamagnetism calculated with Pascal's constants.

Computational Details. DFT geometry optimization and TD-DFT excitation energy calculations were carried out on the molecular structure of **1** (low-spin state ($S = 0$) for Fe^{II}) with the Gaussian 09 (revision A.02) package[2] employing the PBE0 hybrid functional,[3] and applying both a tight self-consistent field convergence criterion ($10^{-9} - 10^{-10}$ a.u.) and an improved optimization threshold (10^{-5} a.u. on average forces). The "Stuttgart/Dresden" basis sets and effective core potentials were used to describe the iron atom,[4] whereas all others atoms were described with the SVP basis sets.[5] The first 80 monoelectronic excitations were calculated for **1**. In all steps, a modelling of bulk solvent effects (solvent = dichloromethane) was included through the Polarisable Continuum Model (PCM),[6] using a linear-response non-equilibrium approach for the TD-DFT step.[7] Molecular orbitals were sketched using the Gabedit graphical interface.[8]
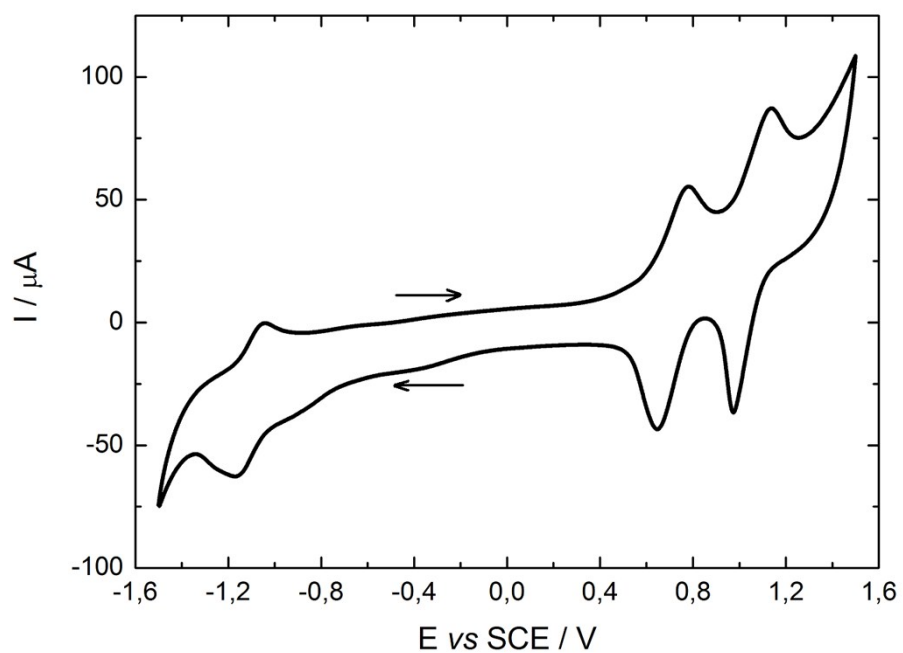
Fig. S1. Cyclic voltammetry of **1** in CH_2Cl_2 at a scan rate of 100 mV·s^{-1} with $[N(C_4H_9)_4]PF_6$ as supporting electrolyte (0.1 M). The potentials were measured *vs* a saturated calomel electrode (SCE); glassy carbon working electrode; Pt wire counter electrode.
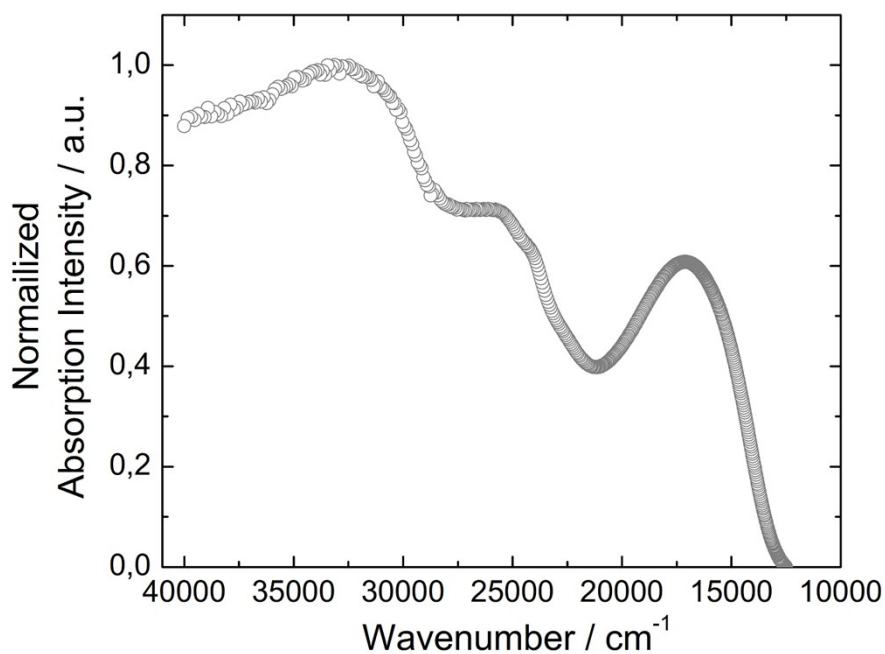

Fig. S2. Experimental solid-state UV-visible absorption spectrum for **1** at room temperature.
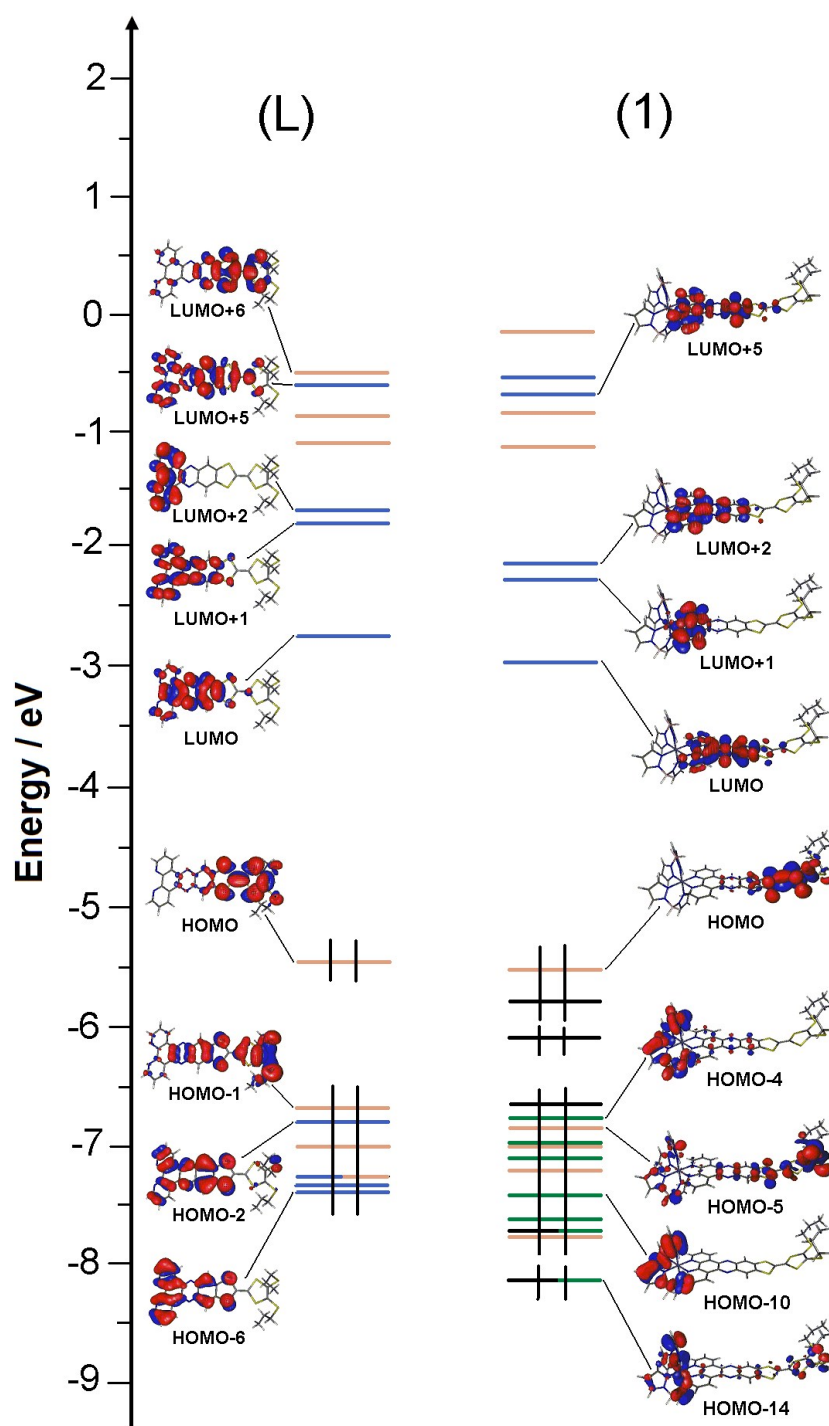
Fig. S3. MO diagram of **L** (left) and **1** (right) with the Fe^{II} ion in its low-spin ($S = 0$) state. Energy levels of the centered TTF donor, dipyridophenazine acceptor and H_2Bpz_2 anions are shown in orange, blue and green, respectively.
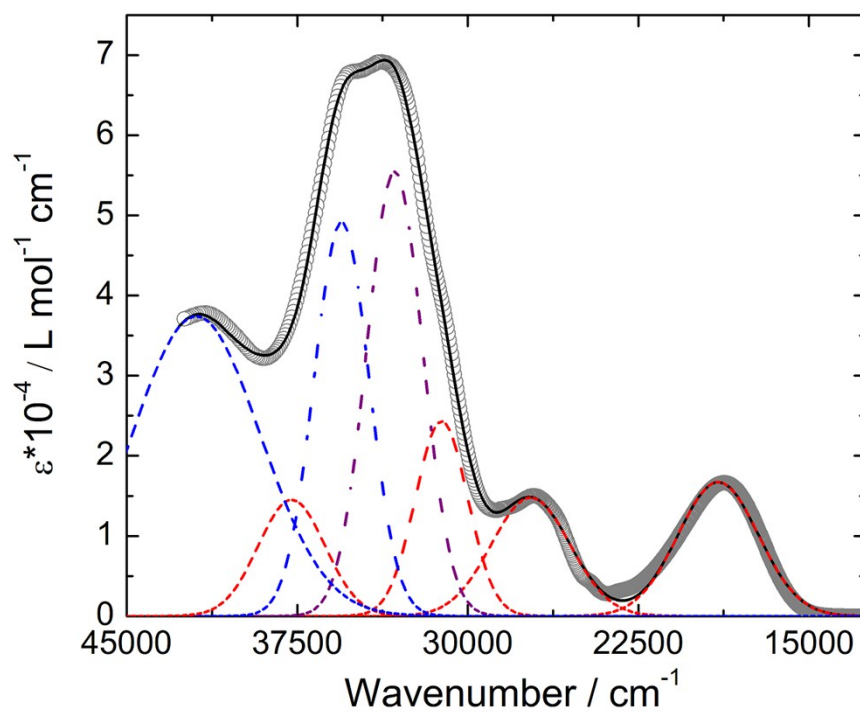
Fig. S4. Experimental UV-visible absorption spectra in CH_2Cl_2 solution of **L** ($c = 4 \times 10^{-5}$ mol L^{-1}) (open gray circles). Respective Gaussian decompositions (dashed lines) and best fit (full black line) ($R^2 = 0.9981$).
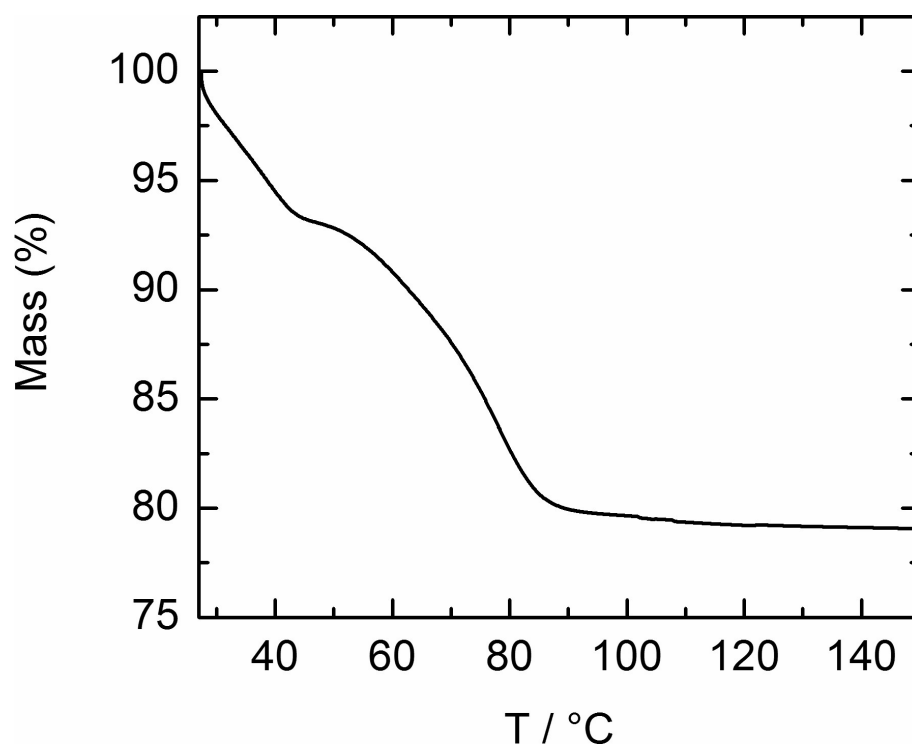
Fig. S5. TGA curve of a fresh sample of **1**·$(CH_2Cl_2)_2$.
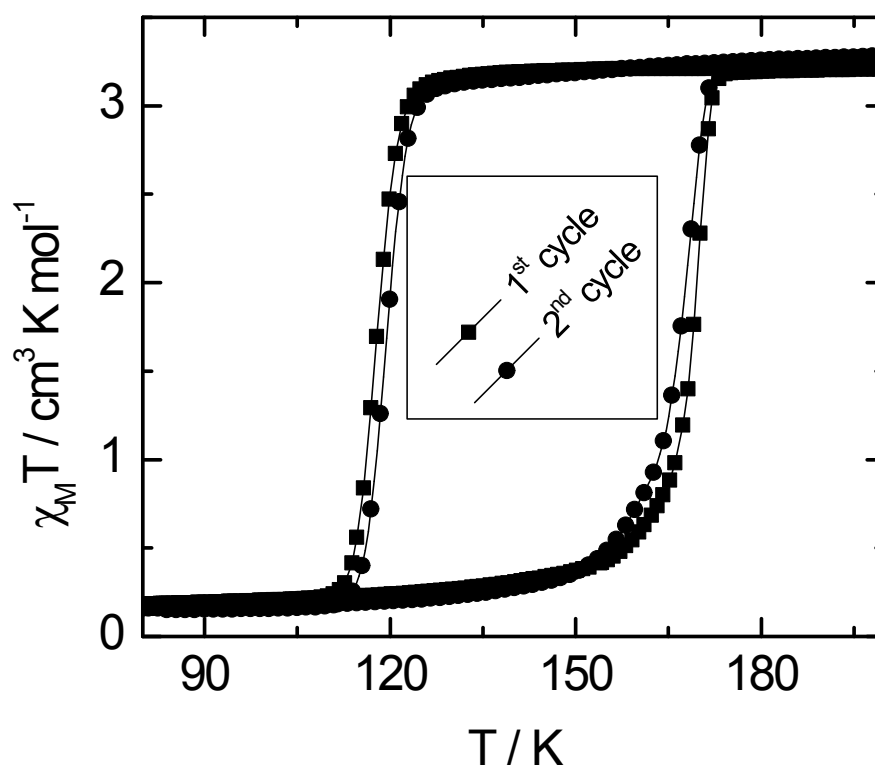
Fig. S6. Two hysteresis loops measured on the same sample of **1**.
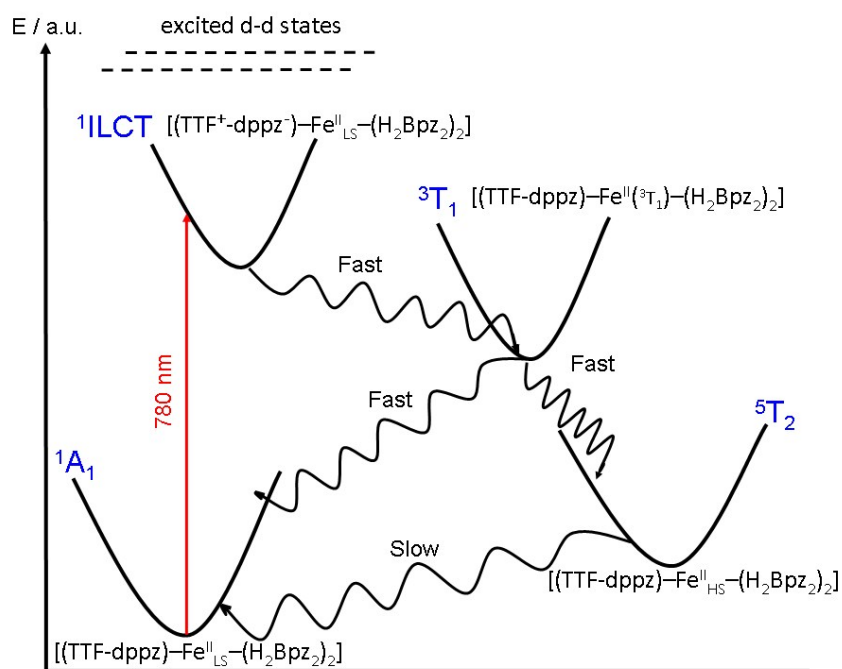
Fig S7. Proposed mechanism for the LIESST effect in **1**.

Fig. S8. PBE+D3+U optimized geometries for the HS ($S = 2$) and LS ($S = 0$) states of **1** with and without solvent molecules.

Table S1. Selected bond lengths (Å) for compound **1**·(CH$_2$Cl$_2$)$_2$ at 150 K.

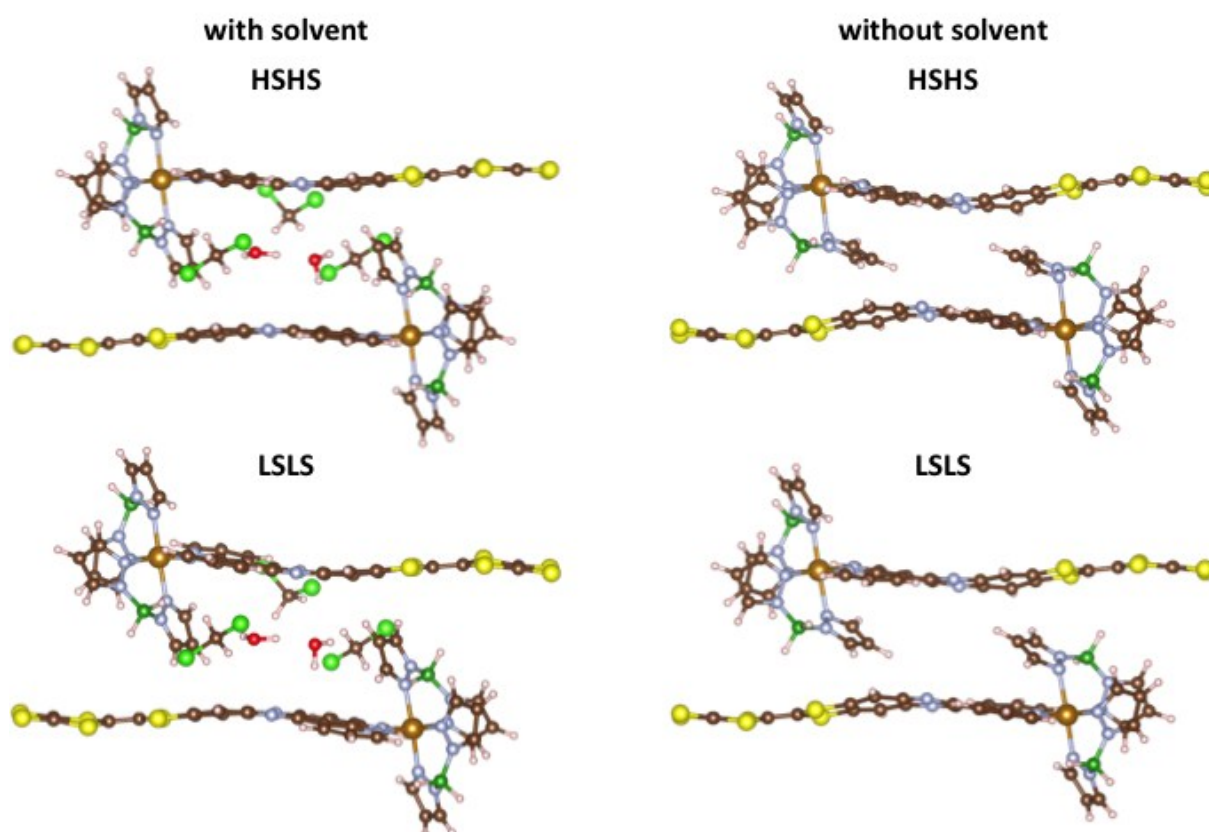| Compound	150 K
Fe1-N1	2.126(3)
Fe1-N2	2.107(3)
Fe1-N3	2.108(3)
Fe1-N4	2.097(3)
Fe1-N5	2.091(3)
Fe1-N6	2.098(3)

Table S2. Experimental and TD-DFT excitation energies and main composition of the low-lying electronic transitions for **L** and **1** (calc for LS). In addition, the charge transfer and the pure intramolecular transitions are reported. IA, IL and H, L represent intramolecular dipyridophenazine (acceptor) transitions or transitions involving orbitals delocalized on the whole ligand and the HOMO and LUMO, respectively. ILCT stands for Intra-Ligand (**L**) Charge Transfer and LLCT for Ligand (H$_2$BPpz$_2$) to Ligand (**L**) Charge Transfer.

	E exp (cm^{-1})	E theo (cm^{-1})	Osc.	Type	Assignment	Transition
	19000	17844	0.42	ILCT	$\pi_{TTF}\rightarrow\pi^*_{dppz}$	H→L (99%)
	27200	27338	0.31	ILCT	$\pi_{TTF}\rightarrow\pi^*_{dppz}$	H-1→L (80%)
	31200	33361	0.11	ILCT	$\pi_{TTF}\rightarrow\pi^*_{dppz}$	H→L+5/+6 (56/33%)
					$\pi_{TTF}\rightarrow\pi^*_{TTF}$	H→L+6 (27%)
(L)*	33200	34504	1.61	IL	$\pi_{TTF}\rightarrow\pi^*_{dppz}$	H→L+5 (31%)
					$\pi_{dppz}\rightarrow\pi^*_{dppz}$	H-2→L+1 (30%)
	35600	35252	0.37	IA	$\pi_{dppz}\rightarrow\pi^*_{dppz}$	H-2→L+1 (29
	37800	36195	0.19	ILCT	$\pi_{TTF}\rightarrow\pi^*_{dppz}$	H-1→L+1/+2 (45/50%)
		36315	0.13			
	41900	42128	0.46	IA	$\pi_{dppz}\rightarrow\pi^*_{dppz}$	H-6→L+2 (68%)
	E exp (cm^{-1})	**E theo (cm^{-1})**	**Osc.**	**Type**	**Assignment**	**Transition**
	18000	16924	0.52	ILCT	$\pi_{TTF}\rightarrow\pi^*_{dppz}$	H→L (98%)
	26800	27116	0.27	ILCT	$\pi_{TTF}\rightarrow\pi^*_{dppz}$	H-5→L (78%)
	31100	31585	0.13	LLCT	$\pi_{H2Bpz2}\rightarrow\pi^*_{dppz}$	H-5/-6→L+1 (19/31%)
						H-4→L+2(56%)
					$\pi_{TTF}\rightarrow\pi^*_{TTF}$	H-13→L (23%)
(1)	32800	32612	0.54	ILCT	$\pi_{TTF}\rightarrow\pi^*_{dppz}$	H→L+5 (59%)
	34900	33732	0.61	LLCT	$\pi_{H2Bpz2}\rightarrow\pi^*_{hfac}$	H-14→L (26%)
				+		H-10/-6→L+1 (78/20%)
				ILCT	$\pi_{TTF}\rightarrow\pi^*_{dppz}$	H-5→L+1 (42%)
						H→L+5/+7 (17/14%)
	38200	/	/	/	/	/
	43200	/	/	/	/	/

* The DFT and TD-DFT calculations of the free ligand **L** were already published[9,10] but they were performed again in order to be fully consistent with the applied method for **1**.

Table S3. Optimized cell parameters within the PBE+D3+U scheme, with and without solvent, in the LS ($S = 0$) and HS ($S = 2$) states of **1**. In the case of the HS molecule with solvent, our calculated results compare very well with the experimental structure.

	no solvent		solvent			
	LS	HS	LS	HS	Exp.	error
a (Å)	12.66058	12.84277	12.75178	12.64236	12.86030	-1.69%
b (Å)	13.37160	13.26478	13.98492	13.92497	14.26060	-2.35%
c (Å)	14.23453	14.29514	14.85214	15.12474	15.79120	-4.22%
α	76.2502	76.3395	76.7781	78.1181	79.1390	-1.29%
β	60.2133	60.3670	59.5691	62.7387	66.2380	-5.28%
γ	64.2719	64.3674	67.4355	68.1179	71.8570	-5.20%

Table S4. Optimized Fe-N bond lengths (Å) within the PBE+D3+U scheme, with and without solvent, in the LS ($S = 0$) and HS ($S = 2$) states of **1**. Numbering is attributed following Figure 1. Again, a close agreement is obtained between calculated and experimental structures in the case of the HS structure with solvent. As an important feature, one can notice the particularly long Fe-N bond (2.42 Å) in the HS state of the compound deprived of solvent.

	no solvent		solvent			
	LS	HS	LS	HS	Exp.	error
Fe-N$_1$	1.97	2.17	1.94	2.15	2.11	+1.90%
Fe-N$_2$	1.95	2.14	1.96	2.17	2.12	+2.36%
Fe-N$_3$	1.98	2.16	1.97	2.10	2.09	+0.48%
Fe-N$_4$	1.98	2.09	1.99	2.13	2.08	+2.40%
Fe-N$_5$	2.00	2.17	1.99	2.12	2.10	+0.95%
Fe-N$_6$	2.10	2.42	2.00	2.15	2.11	+1.90%

References

1. SHELX97 - Programs for Crystal Structure Analysis (Release 97-2). Sheldrick, G. M. Institut für Anorganische Chemie der Universität, Tammanstrasse 4, D-3400 Göttingen, Germany, 1998. SIR97 − A. Altomare, M. C. Burla, M. Camalli, G. L. Cascarano, C. Giacovazzo, A. Guagliardi, A. G. G. Moliterni, G. Polidori, R. Spagna, *J. Appl. Cryst.* 1999, **32**, 115; (b) G. M. Sheldrick, *Acta Crystallogr.* **2008**, **A64**, 112−122; (c) L. J. Farrugia, *J. Appl. Crystallogr.* 2012, **45**, 849−854.

2. M. J. Frisch, G. W. Trucks, H. B. Schlegel, G. E. Scuseria, M. A. Robb, J. R. Cheeseman, G. Scalmani, V. Barone, B. Mennucci, G. A. Petersson, H. Nakatsuji, M. Caricato, X. Li, H. P. Hratchian, A. F. Izmaylov, J. Bloino, G. Zheng, J. L. Sonnenberg, M. Hada, M. Ehara, K. Toyota, R. Fukuda, J. Hasegawa, M. Ishida, T. Nakajima, Y. Honda, O. Kitao, H. Nakai, T. Vreven, J. A. Montgomery, Jr. J. E. Peralta, F. Ogliaro, M. Bearpark, J. J. Heyd, E. Brothers, K. N. Kudin, V. N. Staroverov, R. Kobayashi, J. Normand, K. Raghavachari, A. Rendell, J. C. Burant, S. S. Iyengar, J. Tomasi, M. Cossi, N. Rega, J. M. Millam, M. Klene, J. E. Knox, J. B. Cross, V. Bakken, C. Adamo, J. Jaramillo, R. Gomperts, R. E. Stratmann, O. Yazyev, A. J. Austin, R. Cammi, C. Pomelli, J. W. Ochterski, R. L. Martin, K. Morokuma, V. G. Zakrzewski, G. A. Voth, P. Salvador, J. J. Dannenberg, S. Dapprich, A. D. Daniels, O. Farkas, J. B. Foresman, J. V. Ortiz, J. Cioslowski and D. J. Fox, Gaussian 09 Revision A.02, Gaussian Inc., Wallingford CT, **2009**.

3. (a) J. P. Perdew, K. Burke and M. Ernzerhof, *Phys. Rev. Lett.,* 1996, **77**, 3865; (b) C. Adamo and V. Barone, *J. Chem. Phys.,* 1999, **110**, 6158.

4. M. Dolg, H. Stoll and H. Preuss, *Theor. Chim. Acta,* 1993, **85**, 441.

5. F. Weigend and R. Ahlrichs, *Phys. Chem. Chem. Phys.,* 2005, **7**, 3297-3305.

6. J. Tomasi, B. Mennucci and R. Cammi, *Chem. Rev.,* 2005, **105**, 2999-3094.

7. (a) M. Cossi and V. Barone, *J. Chem. Phys.,* 2001, **115**, 4708; (b) R. Improta, V. Barone, G. Scalmani and M. J. Frisch, *J. Chem. Phys.,* 2006, **125**, 054103.

8. A.-R. Allouche, *J. Comput. Chem.,* **2011**, *32*, 174-182.

9. C. Jia, S.-X. Liu, C. Tanner, C. Leiggener, A. Neels, L. Sanguinet, E. Levillain, S. Leutwyler, A. Hauser and S. Decurtins, *Chem. Eur. J.,* 2007, **13**, 3804-3812.

10. F. Pointillart, J. Jung, R. Berraud-Pache, B. Le Guennic, V. Dorcet, S. Golhen, O. Cador, O. Maury, Y. Guyot, S. Decurtins, S.-X. Liu and L. Ouahab, *Inorg. Chem.,* 2015, **54**, 5384-5397.